Received: 11 December 2019 | Revised: 31 December 2019 | Accepted: 7 January 2020

DOI: 10.1002/ddr.21642

RESEARCH ARTICLE

DDR WILEY

Development and characterization of oxaceprol-loaded poly-lactide-co-glycolide nanoparticles for the treatment of osteoarthritis

Emine Alarçin[1] | Çağlar Demirbağ[2] | Seher Karsli-Ceppioglu[3] | Oya Kerimoğlu[1] | Ayça Bal-Ozturk[4]

[1]Department of Pharmaceutical Technology, Faculty of Pharmacy, Marmara University, İstanbul, Turkey

[2]Department of Analytical Chemistry, Faculty of Pharmacy, Trakya University, Edirne, Turkey

[3]Department of Pharmaceutical Toxicology, Faculty of Pharmacy, Marmara University, İstanbul, Turkey

[4]Department of Analytical Chemistry, Faculty of Pharmacy, İstinye University, İstanbul, Turkey

Correspondence
Emine Alarçin, Department of Pharmaceutical Technology, Faculty of Pharmacy, Marmara University, İstanbul, Turkey.
Email: emine.alarcin@marmara.edu.tr

Funding information
Marmara University Scientific Research Projects Coordination Unit, Grant/Award Number: SAG-A-120613-0234

Abstract

Oxaceprol is well-defined therapeutic agent as an atypical inhibitor of inflammation in osteoarthritis. In the present study, we aimed to develop and characterize oxaceprol-loaded poly-lactide-co-glycolide (PLGA) nanoparticles for intra-articular administration in osteoarthritis. PLGA nanoparticles were prepared by double-emulsion solvent evaporation method. Meanwhile, a straightforward and generally applicable high performance liquid chromatography method was developed, and validated for the first time for the quantification of oxaceprol. To examine the drug carrying capacity of nanoparticles, varying amount of oxaceprol was entrapped into a constant amount of polymer matrix. Moreover, the efficacy of drug amount on nanoparticle characteristics such as particle size, zeta potential, morphology, drug entrapment, and in vitro drug release was investigated. Nanoparticle sizes were between 229 and 509 nm for different amount of oxaceprol with spherical smooth morphology. Encapsulation efficiency ranged between 39.73 and 63.83% by decreasing oxaceprol amount. The results of Fourier transform infrared and DSC showed absence of interaction between oxaceprol and PLGA. The in vitro drug release from these nanoparticles showed a sustained release of oxaceprol over 30 days. According to cell culture studies, oxaceprol-loaded nanoparticles had no cytotoxicity with high biocompatibility. This study was the first step of developing an intra-articular system in the treatment of osteoarthritis for the controlled release of oxaceprol. Our findings showed that these nanoparticles can be beneficial for an effective treatment of osteoarthritis avoiding side effects associated with oral administration.

KEYWORDS

intra-articular injection, nanoparticle, osteoarthritis, oxaceprol, PLGA

1 | INTRODUCTION

Osteoarthritis (OA) is the most common joint disease, affects millions of people in the world, causing a great socioeconomic burden (Rehman et al., 2015; Tellier et al., 2018). OA resulted in chronic pain and physical disability coupled with degeneration in cartilage tissue, subchondral bone and synovium (Kim et al., 2016; Zhang, Ouyang, Dass, & Xu, 2016). Oxaceprol (OXC) is an amino acid derivative (N-acetyl-L-hydroxyproline) getting used in the therapy of degenerative and inflammatory joint diseases including osteoarthritis and rheumatoid arthritis (Bauer et al., 1999; Durg, Lobo, Venkatachalam, Rao, & Bhate, 2019; Veihelmann, Hofbauer, Refior, & Messmer, 2001). Its clinical

efficacy is similar to the conventional nonsteroidal anti-inflammatory drugs but its anti-inflammatory mechanism of action completely different. OXC hinders the inflammatory cascade by preventing leukocyte and granulocyte infiltration into the joints, instead of inhibiting the synthesis of prostaglandins (Herrmann et al., 2000; Kruger, Klasser, Mossinger, & Becker, 2007). It also decreases leukocytes adherence to the blood vessel endothelium, which provide the endothelium integrity, and eventually leads to reduction of macromolecular leakage (Harris, Schropp, & Messmer, 1998). According to in vivo studies, OXC treatment achieved an impressive decrease in the arthritic swelling of the knee and also provided the similar efficacy to diclofenac sodium (Bauer et al., 1999; Herrmann et al., 2000) and ibuprofen (Biehl, Bayer, & Schäferhoff, 1993; Vagt, Kaiser, & Leineweber, 1990) with better safety and tolerability for the treatment of knee and hip OA. Additionally, it has low incidence of gastrointestinal, cardiovascular and renal side effects, compared to NSAIDs (Gu, Chen, Ding, & Zhang, 2011). Its recommended oral dose is 200–400 mg three times daily for a certain period (Ionac, Parnham, Plauchithiu, & Brune, 1996).

Particularly, for the treatment of OA, intra-articular (IA) route is a beneficial choice for the delivery of therapeutics to the affected joint directly (He, Wang, Hu, & Zhao, 2017). High local drug concentrations can be achieved at the site of action with lower administered dose through IA route and hence, it can decrease systemic side effects and drug interactions (Kang, Ko, Kim, & Im, 2014; Maudens et al., 2018). However, IA administration is limited due to practical shortcomings including discomfort, pain and risk of infection (Ho, Kim, Choi, & Kang, 2018). Hence, utilization of polymeric nanoparticles can be beneficial approach to achieve extended drug release and therapeutic levels with a low frequency of injection (Sulistio et al., 2017). Notably, in a recent study, IA injection of OXC provides a significant enhancement in the treatment of OA in osteoarthritis rabbit model (Pawar, Francis, Hota, Peter, & Mitra, 2018).

Among the various biodegradable polymers for fabrication of polymeric nanoparticles, poly-lactide-co-glycolide (PLGA) is a good candidate for the encapsulation of OXC due to its well defined and flexible formulation techniques (Danhier et al., 2012; D. Ding & Zhu, 2018). PLGA is also approved by the US Food and Drug Administration (FDA) and European Medicine Agency (EMA) to utilizing in drug-delivery purposes (Chereddy, Vandermeulen, & Préat, 2016; Jose et al., 2014) due to its biocompatible, biodegradable, and nontoxic properties (Eren et al., 2016; Ji et al., 2017). Moreover, the degradation period of PLGA can be varied from days to months due to alteration in its molecular weight and copolymer ratio (Martins, Sousa, Araújo, & Sarmento, 2018). For their use in IA route, previously, Horisawa and co-workers developed PLGA nanoparticles for IA injection, and achieved prolonged efficacy in both arthritic rabbit and rat models (Horisawa, Hirota, et al., 2002; Horisawa, Kubota, et al., 2002).

Here, we aimed to design and characterize OXC loaded PLGA nanoparticles for IA injections in the treatment of OA to provide sustained release of OXC and minimize injection frequency to improve patient compliance. PLGA nanoparticles were fabricated by double-emulsion method due to hydrophilicity of OXC (S. Ding, Serra, Vandamme, Yu, & Anton, 2018; Sipahigil et al., 2012). Herein, first, formulation variables including polymer amount, speed and duration of homogenization were investigated to determine the optimum nanoparticle formulation. Subsequently, different amounts of oxaceprol (30, 60, 150 mg) were encapsulated into this optimized nanoparticle formulation to see drug carrier capacity of nanoparticles as well as the efficacy of drug amount on nanoparticle characteristics such as particle size, zeta potential, morphology, drug entrapment, and drug release. Meanwhile, a high performance liquid chromatography (HPLC) method was developed to determine the encapsulation efficiency and release behavior of OXC nanoparticles. This proposed HPLC method was straightforward, easy and quick to apply in pharmaceutical analysis to determine OXC amount. Finally, the biocompatibility of these nanoparticles was demonstrated using 2,3-bis(2-methoxy-4-nitro-5-sulfophenly)-5-([phenylamino] carbonyl)-2H-tetrazolium hydroxide test (XTT).

2 | MATERIALS AND METHODS

2.1 | Materials

OXC (molecular weight of 173.17 g/mol), PLGA with a 50:50 copolymer ratio (molecular weight of 30–60 kDa), and 98% hydrolyzed polyvinyl alcohol (PVA) (molecular weight of 72 kDa) was purchased from Sigma Aldrich Inc. (St. Louis, MO). The XTT kit was provided from Biological Industries Ltd. (Kibbutz Beit-Haemek, Israel). RPMI medium, fetal bovine serum and penicillin–streptomycin were obtained from Gibco (Grand Island, NY). All other reagents used were of analytical grade.

2.2 | Preparation of PLGA nanoparticles

OXC loaded PLGA nanoparticles were fabricated by double-emulsion (W1/O/W2) solvent evaporation method, described elsewhere, using different amounts of polymer and drug (Alarçin et al., 2018). Briefly, a 2 ml aqueous internal phase containing 30, 60, or 150 mg OXC was emulsified in a 5 ml methylene chloride solution containing 300 mg PLGA by homogenization (IKA T18 digital ULTRA-TURRAX, Germany) at 12,000 rpm for 3 min. This primary emulsion was poured into 10 ml of a 1.5% (w/v) aqueous PVA solution and followed by homogenization at 8,000 rpm for 1 min. The obtained double emulsion was dispersed in 150 ml of a 0.5% (w/v) PVA solution under agitation for 2 h using a propeller mixer (Janke & Kunkel IKA-WERK RE16, Germany) to achieve completely evaporation of the organic solvent. The resultant particles were separated by centrifugation at 30,000*g* for 30 min at 4°C and washed three times with distilled water to remove unloaded OXC and residual PVA. Finally, the obtained nanoparticles were lyophilized (Christ, Alpha 1-2 LD Plus, Germany) for 24 hr.

2.3 | Nanoparticle morphology

The morphology of lyophilized nanoparticles was analyzed by a scanning electron microscope (SEM) (JEOL/JSM-6335F, Japan) at an

accelerating voltage of 10 kV. The nanoparticles were coated with 10 nm palladium/gold under vacuum before SEM analyses.

2.4 | Nanoparticle size and zeta potential measurement

The mean particle diameter, polydispersity index and zeta potential of nanoparticles were determined by dynamic laser light scattering at room temperature (Malvern Zetasizer Nano ZS, UK).

2.5 | Infrared spectrophotometry (FTIR)

The Fourier transform infrared (FTIR; SHIMADZU, FTIR-8300, Japan) analysis was employed to determine the chemical interaction between OXC and PLGA. IR spectra of OXC, PLGA, physical mixture (1:1), and fabricated nanoparticles were investigated at 400–4,000 cm^{-1} wavelength.

2.6 | Differential scanning calorimetry

Differential scanning calorimetry (DSC) thermal analysis was conducted to determine the physical status of OXC entrapped in nanoparticles. OXC, PLGA, physical mixture (1:1), and fabricated nanoparticles were heated to 350°C with the heating rate of 10°C min^{-1} under a nitrogen atmosphere using Perkin Elmer, Jade. Alumina was employed as a reference material.

2.7 | The production yield (%)

Nanoparticles were weighed accurately after lyophilization procedure, and the production yield (%) was calculated using following equation (Gupta et al., 2010):

$$\text{The production yield}\,(\%) = \frac{\text{Mass of nanoparticles recovered}}{\text{Mass of polymer; drug; and other excipients used}} \times 100$$

2.8 | High performance liquid chromatography

2.8.1 | Chromatographic conditions

The concentration of oxaceprol was determined using HPLC system consisted of Agilent 1200 series pump, diode array detector, thermostatic column compartment, Agilent 1100 series automatic sample injector, and Chemstation data acquisition program (Agilent Technologies, Santa Clara, CA). Hichrom Kromasil C8 (250 × 4.6 mm, 5 μm, 100 Å) analytical column was employed for the analysis. The mobile phase comprising of 40 mM, phosphate buffer solution adjusted to pH = 2.6 using o-phosphoric acid (A) and acetonitrile (B). The elution of oxaceprol was achieved with linear gradient elution of mobile phase as followed (v/v) 0 to 25% B, 0–7 min; 25 to 0% B, 7–9.5 min with 0.6 ml/min flowrate and 5 μl injection volume at 25 ± 0.5°C. Detection of oxaceprol was carried out at 208 nm detector wavelength. Sample solutions centrifuged at 30,000*g* for 30 min and filtered through 0.45 μm HDPE syringe filters before injections.

2.8.2 | Method validation

The proposed HPLC procedure was validated according to International Conference on Harmonization guidelines in terms of linearity, limit of detection and quantification, precision, and accuracy of the method (ICH Harmonised Tripartite Guideline, 2005.

Linearity

The linearity of calibration curve was obtained by six concentrations of oxaceprol standard (4.00, 8.00, 12.00, 16.00, 24.00, 32.00 μg/ml) with triplicate injections in three different days. Each peak area were plotted against concentrations and the linearity described by least squares regression analysis.

Limit of detection and limit of quantification

Limit of detection (LOD) and limit of quantification (LOQ) calculated by using signal to noise (S/N) approach. The oxaceprol concentration with S/N ratio above three was qualified as LOD and S/N above 10 considered as LOQ. The oxaceprol test solutions were injected into system in triplicate in three different days.

Precision of method

Precision of method was performed by intraday (n = 3) and interday (three injections in three different day in 1 week, n = 9) assays and results reported in terms of relative *SD*. The concentrations of injected solutions determined as low, medium, and high levels of the calibration curves.

Accuracy of method

Accuracy (recovery) of HPLC method was determined by standard addition method at three levels (80, 100, and 120%). Known amount of oxaceprol was added to preanalyzed nanoparticle sample solution and injected three times for each level.

2.9 | Encapsulation efficiency and drug loading

To determine drug content, 5 mg of nanoparticles were dissolved in 10 ml of DCM and then 10 ml of deionized water/methanol (1:1) was added. The final solution was shaken on a shaker for 24 hr to leach out oxaceprol entirely. This solution was centrifuged at 30,000*g* for 30 min for obtaining water phase to measure drug concentration. An aliquot of 5 μl was used for HPLC analysis, as described before.

The oxaceprol content of nanoparticles was expressed as drug encapsulation efficiency (%) and drug loading (%) according to the following equations (Barakat & Ahmad, 2008):

$$\text{Encapsulation efficiency}\,(\%) = \frac{\text{Actual drug content in nanoparticles}}{\text{Theoretical drug content}} \times 100$$

$$\text{Drug loading}\,(\%) = \frac{\text{Mass of drug in nanoparticle}}{\text{Mass of nanoparticle recovered}} \times 100$$

2.10 | In vitro drug release and release kinetic

Oxaceprol release studies were carried out by incubating nanoparticles in phosphate buffer (PBS, pH 7.4) at 37°C in a water bath under constant agitation at 100 rpm. At predetermined time intervals, the tubes were centrifuged at 30,000*g* for 30 min at 4°C. Then supernatant was separated for analysis. The same volume of fresh buffer was replaced into the release tube immediately after each sampling to maintain the oxaceprol concentration within sink conditions. The supernatant was analyzed for oxaceprol content by the HPLC method described previously.

The release mechanisms of oxaceprol from nanoparticles were determined by evaluation of kinetic models, including zero order, first order, Korsmeyer–Peppas, Higuchi, and Hixson–Crowell (see Supporting Information Section 1 for details). Determination coefficient (R^2) of the first 60% of drug release is used to assess the best-fit model of drug release (England, Miller, Kuttan, Trent, & Frieboes, 2015).

2.11 | In vitro cytotoxicity studies

The cytotoxic activity of free oxaceprol, oxaceprol-loaded nanoparticles, and blank nanoparticles was evaluated using the colorimetric XTT assay. Human lymphoblastoid cell lines (LCLs) from healthy consenting donors, provided from the National Laboratory for the Genetics of Israeli Populations (NLGIP; http://yoran.tau.ac.il/nlgip/), were used for cell culture experiments. Cells were cultured in RPMI medium supplemented with 10% fetal bovine serum, antibiotics (100 U/ml penicillin; 100 μg/ml streptomycin) and 2 mM extra L-glutamine (final concentration of 4 mM L-glutamine) at 5% CO_2 and 37°C for 24 h. Briefly, LCLs were seeded in 96-well plate at a concentration of approximately 2×10^5 cells/ml in culture media. The cells were further incubated with drug loaded and drug free nanoparticles at equivalent drug concentration for 1, 10, 50 and 100 μg/ml in a volume of 10 μg PBS for 72 hr (n = 4). The XTT experimental procedure was conducted according to kit protocol and (Morag, Kirchheiner, Rehavi, & Gurwitz, 2010). The absorbance of the free drug and nanoparticles was measured at a wavelength of 450 nm (655 nm background) by using an Epoch microplate spectrophotometer (BioTek Instruments).

2.12 | Stability studies of nanoparticles

The physical stability of the lyophilized nanoparticle was investigated after 6 month storage comparing to initial findings. Lyophilized nanoparticles were stored at 5 ± 2°C (refrigerator) or 25 ± 2°C and 60% relative humidity (RH). The particle size, polydispersity index, zeta potential, and drug content were determined for stability evaluation. HPLC was performed for detecting drug content as described previously.

2.13 | Statistical analysis

The results were presented as means ± *SD*s. in vitro characterization studies were carried out in triplicate. In vitro cytotoxicity studies conducted in four times. The Student's *t*-test was conducted for statistical analysis and the threshold for statistical significance was at $p < .05$.

3 | RESULTS AND DISCUSSION

3.1 | Preparation of oxaceprol-loaded PLGA nanoparticles

PLGA nanoparticles were successfully fabricated to obtain a matrix type solid structure by employing W/O/W double-emulsion solvent evaporation method. PVA, a FDA approved surfactant used in several delivery systems, was used as a stabilizer during homogenization procedure for the generation of nanoemulsion droplets without coalesces (Karagoz et al., 2012; Martinez, Andrade, Durán, & Cavalitto, 2017). To form nanoparticles, firstly an o/w primary emulsion was prepared, and then droplet size was reduced using a homogenizer. In this method, hydrophilic drug was dissolved in the inner aqueous phase of the emulsion to achieve high encapsulation efficiency and prolong drug release. The obtained primary emulsion was diluted in a second aqueous phase under homogenization, which resulted in release of the energy for the formation of the particles (Song et al., 2008). Subsequently, dichloromethane was evaporated under constant agitation for the solidification of obtained particles. Various formulation parameters including polymer amount, homogenization speed and duration were investigated to determine the optimized formulation coded with NP (see Supporting Information Section 2 for details).

Subsequently, drug carrying capacity of PLGA nanoparticles was examined by varying the amount of OXC to a constant amount of polymer. For this purpose, three different amounts of OXC (30,

TABLE 1 Formulation characteristics of free and OXC loaded PLGA nanoparticles

Code	Polymer to drug ratio	Mean particle size (nm ± *SD*)	Polydispersity index (nm ± *SD*)	Zeta potential (mV ± *SD*)	Production yield (% ± *SD*)	Encapsulation efficiency (% ± *SD*)	Drug loading (% ± *SD*)
NP	–	93 ± 21	0.38 ± 0.09	−21 ± 1.2	72.42 ± 4.1	–	–
LNP	1:0.1	229 ± 34	0.3 ± 0.14	−23 ± 1.1	69.05 ± 3.8	63.83 ± 2.1	8.94 ± 0.2
MNP	1:0.2	335 ± 66	0.3 ± 0.1	−22 ± 1.3	58.25 ± 2.6	57.36 ± 2.3	16.22 ± 1.8
HNP	1:0.5	509 ± 52	0.26 ± 0.11	−21 ± 1.1	35.03 ± 2.1	39.73 ± 3.6	56.31 ± 3.7

Note: Particle sizes were given as number.
Abbreviations: HNP, nanoparticles including high amount of OXC; LNP, nanoparticles including low amount of OXC; MNP, nanoparticles including medium amount of OXC; NP, free PLGA nanoparticles.

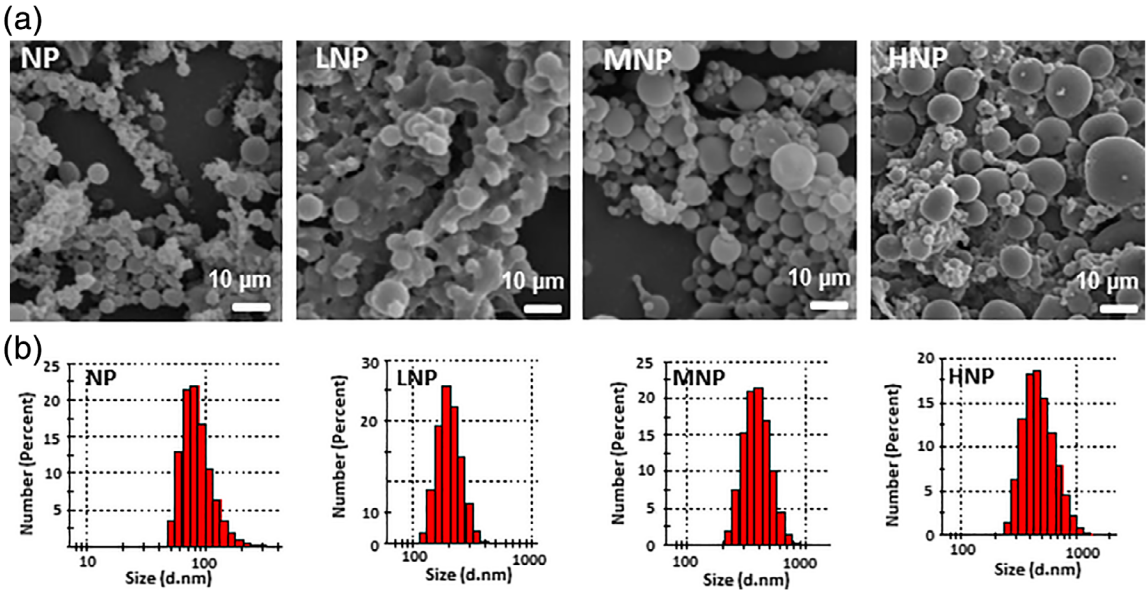

FIGURE 1 (a) Scanning electron micrographs and (b) particle size distribution of PLGA nanoparticles including NP (for oxaceprol free nanoparticles), LNP (for nanoparticles including low amount of OXC) MNP (for nanoparticles including medium amount of OXC), and HNP (for nanoparticles including high amount of OXC) coded formulations

60, and 150 mg) loaded into nanoparticles with a certain polymer to drug ratio 1:0.1, 1:0.2, and 1:0.5, respectively. Herein, the formulation codes were determined as LNP (for nanoparticles loaded with low amount of OXC), MNP (for nanoparticles loaded with medium amount of OXC), HNP (for nanoparticles loaded with high amount of OXC), and also NP (for OXC free nanoparticles).

3.2 | Surface morphology, particle size, and zeta potential

As shown in Figure 1a, SEM images demonstrated that NP, LNP, MNP, and HNP coded PLGA nanoparticles had spherical shape with a smooth surface morphology.

According to DLS measurements, average particle sizes of NP, LNP, MNP, and HNP were found to be 93 ± 21, 229 ± 34, 335 ± 66, and 509 ± 52 nm, respectively (Table 1, Figure 1b). Notably, particle sizes were increased with an increase in drug amount probably due to more viscous aqueous phase based upon high amount of oxaceprol resulted in incomplete dispersion of the phases (Mainardes & Evangelista, 2005). Zeta potential values of particles were in range between −23 and −21 mV indicating the stability of nanoparticles due to electrostatic repulsion forces which prevent particle aggregation (Alarçin et al., 2018).

3.3 | Physiochemical properties of nanoparticles

Figure 2a demonstrates the FTIR spectra of PLGA, OXC, physical mixture of PLGA and OXC (1:1), and OXC loaded formulations. IR spectra of OXC showed C—H stretching at 2,944 and 2,870 cm^{-1}, C—N stretching at 1,280 cm^{-1}, and C═O stretching at 1,608 and 1,735 cm^{-1}. The characteristic peak of PLGA was observed at 1,746 cm^{-1} due to C═O stretching. IR spectra indicated that the physical mixture showed no differences in the position of the main peaks of OXC, PLGA, and PLGA nanoparticles exhibited the same characteristic peaks of polymer.

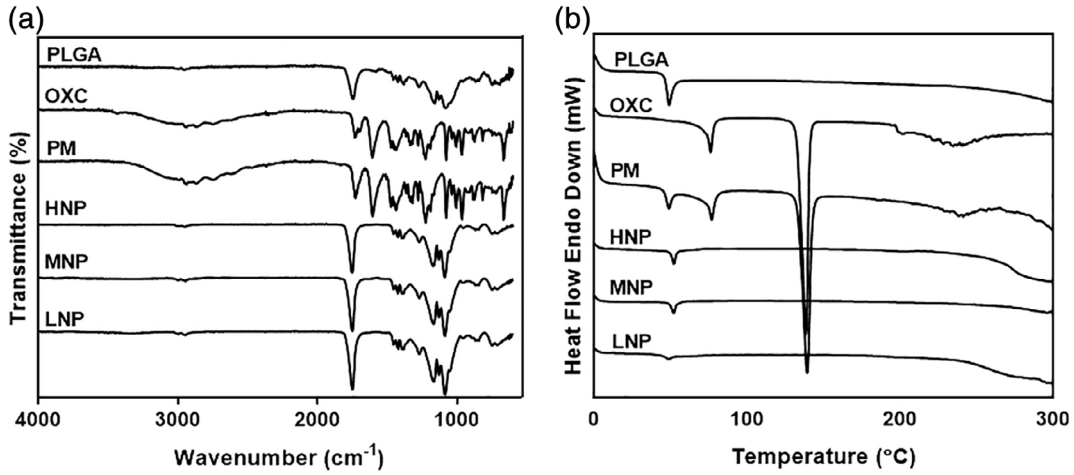

FIGURE 2 (a) FTIR spectra and (b) DSC thermograms of PLGA, oxaceprol, PM (physical mixture of PLGA and oxaceprol) (1:1), HNP (for nanoparticles including high amount of OXC), MNP (for nanoparticles including medium amount of OXC), and LNP (for nanoparticles including low amount of OXC) coded formulations

A DSC analysis was performed for the investigation of physical status of OXC in the formulated PLGA nanoparticles, and also PLGA–OXC interaction during nanoparticle preparation process. Figure 2b shows DSC thermograms of PLGA, OXC, PLGA/OXC physical mixture (1:1), OXC-loaded PLGA nanoparticles (HNP, MNP, and LNP). It is demonstrated that two endothermic peaks were found for OXC at 75.97 and 137.19°C, and one endothermic peak for PLGA at 48.58°C. In regard to the physical status of OXC in the PLGA nanoparticles fabricated, the endothermic peaks of the OXC were not observed in the thermograms of OXC-loaded PLGA nanoparticles. This refers that OXC was not physically adsorbed onto the surface of nanoparticle and entrapped in PLGA matrix (Holgado et al., 2008). There was no drug melting peak observable in the DSC curve of all OXC loaded PLGA nanoparticles indicating that OXC was present in a noncrystalline state (Corrigan & Li, 2009; Souillac & Rytting, 1999). With accordance with FTIR results, it can be concluded that there is no interaction between OXC and PLGA; and also OXC was entrapped into polymer matrix successfully.

3.4 | HPLC validation

To assess OXC amount in nanoparticles, an effective, simple and rapid HPLC method was developed for the first time. Method validation was employed to prove that the newly developed method is applicable for its proposed use (ICH Harmonised Tripartite Guideline, 2005). The results of method validation were summarized at Figure S2a.

The linearity of calibration curve was investigated between 4 and 32 μg/ml. The calibration curve was obtained by plotting peak area ratio against concentrations. The regression equation was found $y = 16.766x - 20.65$ and the regression coefficient (R^2) was found 0.9998 according to regression analysis indicating a strong correlation between the peak areas and concentrations (Figure S2b).

LOD and LOQ were evaluated by using signal/noise (S/N) ratio wherein the OXC concentration of S/N ratio above three was considered as LOD and S/N above 10 determined as LOQ. LOD and LOQ results of oxaceprol were 0.75 and 1.4 μg/ml, respectively.

The intraday and interday precision were evaluated on three different concentration levels. The relative standard deviation (*RSD*) of interday precision was 0.72% and the *RSD* of intraday precision was 1.19%. Therefore, proposed method demonstrated the suitable precision with *RSD* lower than 2%. Additionally, the retention time (RT) was provided with the injection of the standard solution in series ($n = 10$) and determined as 9.47 ± 0.01.

The accuracy was obtained by the recovery of known amounts of OXC at three levels. The accuracy percentages were calculated by comparing the concentration values found for each level to the theoretical values assayed (supposed to be 100%). Accuracy percentages were found to be between 99.78 and 100.53%. Particularly, the *RSD* of obtained results were lower than 2 which fulfills the accuracy criteria of FDA (Shabir, 2003).

3.5 | The production yield, drug loading, and entrapment efficiency

The production yield of NP, LNP, MNP, and HNP were determined as 72.42% ± 4.1, 69.05 ± 3.8, 58.25 ± 2.6, and 35.03 ± 2.1, respectively. To evaluate the drug entrapment capacity of PLGA nanoparticles, the encapsulation efficiency and drug-loading capacity were determined. Notably, OXC entrapment efficiency and drug loading (%) was governed by initial OXC amount and particle size. Entrapment efficiency changed from 63.83 to 39.73% by the increase in initial drug amount from 30 to 150 mg. However, drug loading (%) increased from 8.94 to 56.3% by increasing drug amount as shown in Table 1. The solid polymer matrix has a limited capacity to entrap certain drug molecule. Hence, further increase in the OXC concentration exceeding a threshold resulted in more drug loss during fabrication process and led to decrease in encapsulation efficiency (Bal Öztürk, Cevher, Pabuccuoğlu, & Özgümüş,

2018; Dong & Feng, 2004). Furthermore, the encapsulation efficiency found to be enhanced with the increasing diameter of nanoparticles in the accordance with literature (Mainardes & Evangelista, 2005).

3.6 | In vitro drug release and release kinetic

In drug release studies, a biphasic release pattern was obtained from LNP, MNP and HNP formulations with an initial burst release, followed by a sustained release of remaining drug as seen in Figure 3. The initial burst release of oxaceprol from nanoparticles was due to both from molecules weekly bound to the surface of the nanoparticles and the diffusion of molecules located near to surface of nanoparticles (Sokol et al., 2018). Particularly, burst release was beneficial to obtain initial therapeutic concentration of OXC. Herein, the higher OXC amount led to higher initial burst release and 50% of OXC release was accomplished after 2, 4, and 9 days for HNP, MNP, and LNP, respectively. After day 30, the cumulative release percentages from HNP, MNP, and LNP were calculated as 89.57, 78.93, and 63.21%, respectively. Based on these results, OXC was released in a sustained manner for all formulations which is attributed to the slow degradation rate of PLGA (Anderson & Shive, 2012). Overall, it is important to note that OXC release rate was affected by the amount of entrapped drug and particle size. The higher drug-loading capacity resulted in a faster release rate due to concentration gradient and thus nanoparticles with lower OXC amounts achieved a release trend in a more sustained manner. Additionally, according to previous literature degradation rate of larger particles was fastest because of both autocatalytic effects and length of diffusion path (Dillen, Vandervoort, Van den Mooter, & Ludwig, 2006; Dunne, Corrigan, & Ramtoola, 2000). It is also corresponded well with the present study because larger nanoparticles (HNP) degraded fast and thus resulted in fastest release.

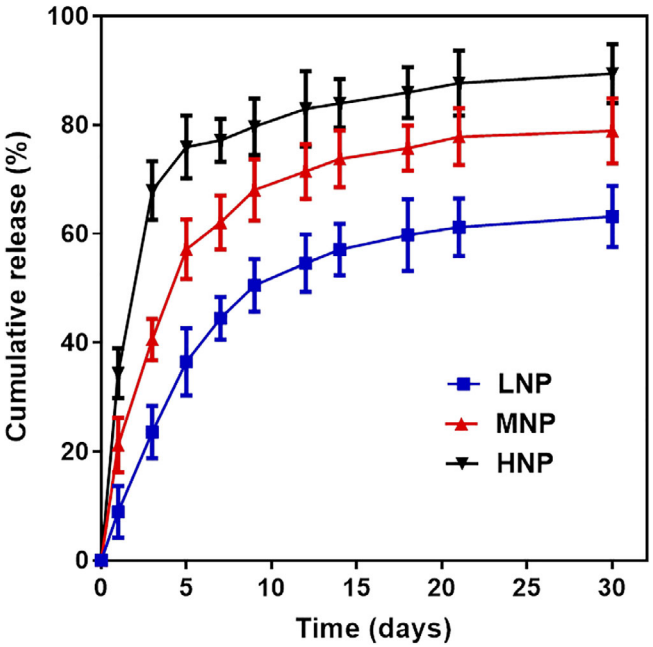

FIGURE 3 Cumulative release of oxaceprol from HNP, MNP, and LNP coded PLGA nanoparticles in pH 7.4 phosphate buffer for 1 month at 37°C. HNP, MNP, and LNP stands for including high, medium, and low amount of OXC, respectively. Results are presented as means ±*SD*s (n = 3)

OXC release kinetics from PLGA nanoparticles were fitted into kinetic models, including zero order, first order, Korsmeyer–Peppas, Higuchi, and Hixson–Crowell. The first 60% of drug release is used to determine the best-fit model (England et al., 2015). The kinetic model was determined according to determination coefficient. Table 2 displays determination coefficient values for each kinetic model. The release kinetics of HNP, MNP, and LNP were best fit into Higuchi and Korsmeyer–Peppas model with higher correlation value rather than others. Higuchi square root model refers to diffusion controlled release (Chaudhary & Kumar, 2014). The release exponent value (n) obtained from Korsmeyer–Peppas, was between 0.5717 and 0.6673, indicating "Non-Fickian Diffusion Transport" mechanism of drug release. It describes the release mechanism based on both diffusion and erosion. Notably, the diffusion could be ascribed to the generation of potential gradient of drug molecule, while erosion attributed to stress conditions (Altındal & Gümüşderelioğlu, 2016).

3.7 | Cytotoxicity

The cytotoxicity of drug-delivery systems is an important parameter for their potential application. In this respect, the cellular viabilities of OXC loaded nanoparticles were determined by XTT assay and compared with a free OXC solution and OXC free nanoparticles at various concentrations including 1, 10, 50, and 100 μg/ml to evaluate dose

TABLE 2 Kinetic parameters obtained from model equations for OXC release from LNP, MNP, and HNP coded PLGA nanoparticles

	Release models									
	Zero order		First order		Korsmeyer–Peppas		Higuchi square root		Hixson–Crowell	
Code	r^2	k_0 (hr^{-1})	r^2	k_1 (hr^{-1})	r^2	n	r^2	k ($\%hr^{-0.5}$)	r^2	k ($\%hr^{-1/3}$)
LNP	0.8522	0.1371	0.9174	0.0009	0.954	0.6673	0.9691	3.211	0.8972	0.0029
MNP	0.9231	0.3606	0.9708	0.0025	0.9911	0.5717	0.992	4.9969	0.958	0.0076
HNP	0.9633	0.9193	0.9953	0.0067	0.9969	0.6152	0.9986	7.312	0.9916	0.0199

Abbreviations: HNP, nanoparticles including high amount of OXC; LNP, nanoparticles including low amount of OXC; MNP, PLGA nanoparticles including medium amount of OXC; NP, Free PLGA nanoparticles.

TABLE 3 Effects of storage conditions after 6 months on the mean particle sizes as number, and drug-loading values of LNP, MNP, and HNP coded PLGA nanoparticles

	Mean particle size (nm) ± *SD*			Drug loading (%) ± *SD*		
Code	Initial values	5°C	25°C/60% RH	Initial values	5°C	25°C/60% RH
LNP	229 ± 34	279 ± 110	335 ± 92	8.94 ± 0.2	7.81 ± 1.2	6.43 ± 1.7
MNP	335 ± 66	424 ± 123	479 ± 134	16.22 ± 1.8	14.96 ± 2.4	13.12 ± 2.7
HNP	509 ± 52	589 ± 204	620 ± 244	56.31 ± 3.7	52.7 ± 4.9	51.61 ± 5.4

Abbreviations: NP, free PLGA nanoparticles; LNP, nanoparticles including low amount of OXC; MNP, PLGA nanoparticles including medium amount of OXC; HNP, nanoparticles including high amount of OXC.

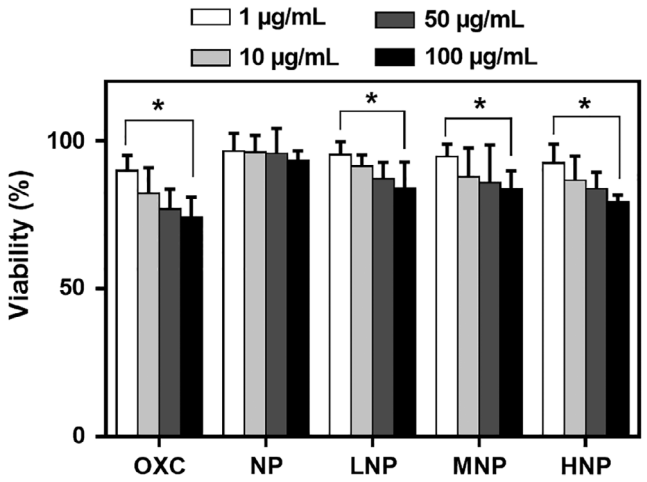

FIGURE 4 Cell viability of LCLs cells incubated with OXC, OXC free PLGA nanoparticles (NP), and OXC loaded PLGA nanoparticles (LNP, MNP, and HNP) at 1, 10, 50, and 100 µg/ml OXC concentrations and 37°C for 72 hr. LNP, MNP, and HNP stands for including low, medium, and high amount of OXC, respectively. Results are presented as means ± *SD*s ($n = 4$) (*$p < .05$)

depended response (Figure 4). LCLs from unrelated healthy individuals have been utilized as useful tools for searching drug-response biomarker (Morag et al., 2010; Vincent et al., 2012). The cellular viability of free OXC was 89.84 and 75.2% for 1 and 100 µg/ml concentrations, respectively. The cellular viability of drug free PLGA nanoparticles was more than 90% even at the highest concentration indicating the biocompatibility of PLGA and no residue of organic solvent with an accordance to previous literature (Tansık, Yakar, & Gündüz, 2014). Moreover, for each concentration level, cells treated with oxaceprol-loaded nanoparticles exhibited higher viability than those cells treated with free oxaceprol. The viability of cells was above 80% for OXC loaded formulations (LNP, MNP, HNP) even at 100 µg/ml concentrations. It was clearly indicated that OXC loaded PLGA nanoparticles had no cytotoxicity and exhibited high biocompatibility.

3.8 | Stability

To evaluate the physical stability of lyophilized oxaceprol-loaded PLGA nanoparticles, nanoparticles were stored at 5 ± 2 and 25 ± 2°C for 6 months period. Subsequently, particle size, zeta potential, and loading efficiency were evaluated compared to initial findings (Table 3). There was no significant difference in initial values of particle sizes over storage for 6 months at 5 and 25°C ($p > .05$). Polydispersity indexes were less than or equal to 0.6 for all formulations. Lyophilized LNP, MNP, HNP coded nanoparticle formulations can be redispersible in both water and PBS easily even after 6 months for both 5 and 25°C. To further confirm oxaceprol content under different storage conditions, drug-loading percentages were assessed over 6 months using HPLC. OXC amount was >95% for all formulations compared to initial OXC amount ($p > .05$). Based on these findings, these nanoparticle formulations were resuspendable with a suitable particle size and drug content for IA injection in the OA treatment even after 6 months.

4 | CONCLUSION

OXC had been shown as the effective choice in the treatment of OA avoiding side effects of NSAIDs. However, it is difficult to achieve therapeutic concentration of drugs in the joint. Thus, localized IA delivery of therapeutics can be a beneficial strategy in the management of OA. In this study, a hydrophilic drug, oxaceprol was successfully entrapped into PLGA nanoparticles using W/O/W double-emulsion solvent evaporation method for IA injection in the treatment of OA. Moreover, a straightforward and rapid HPLC method was established, and also validated for the quantification of OXC for further drug loading and release studies. Different amount of OXC was entrapped into a constant amount of polymer matrix in order to investigate the drug carrying capacity of nanoparticles. The results indicated that drug release kinetics was closely associated with drug loading and particle size. Higher drug loading and larger particle size resulted in fastest drug release. Finally, according to XTT analysis on LCLs, developed OXC loaded nanoparticles had no cytotoxicity. The present study introduces an initial step of developing nanoparticles for IA injection in the OA treatment and it was expected that after further in vivo studies, these nanoparticles could be used in clinic for a safe and effective therapy of OA.

ACKNOWLEDGMENTS

This project has been supported by Marmara University Scientific Research Projects Coordination Unit under grant number SAG-A-

120613-0234. The authors would like to gratefully thank Prof. David Gurwitz for sharing human lymphoblastoid cell lines from the collection of the National Laboratory for the Genetics of Israeli Populations biobank at Tel Aviv University, Israel, and the anonymous donors of this cell line collection for their dedication to scientific research.

CONFLICT OF INTEREST

The authors declare no conflict of interest.

ORCID

Emine Alarçin https://orcid.org/0000-0003-1352-5239

REFERENCES

Alarçin, E., Lee, T. Y., Karuthedom, S., Mohammadi, M., Brennan, M. A., Lee, D. H., … Zhang, Y. S. (2018). Injectable shear-thinning hydrogels for delivering osteogenic and angiogenic cells and growth factors. *Biomaterials Science*, *6*(6), 1604–1615.

Altındal, D. Ç., & Gümüşderelioğlu, M. (2016). Melatonin releasing PLGA micro/nanoparticles and their effect on osteosarcoma cells. *Journal of Microencapsulation*, *33*(1), 53–63.

Anderson, J. M., & Shive, M. S. (2012). Biodegradation and biocompatibility of PLA and PLGA microspheres. *Advanced Drug Delivery Reviews*, *64*, 72–82.

Bal Öztürk, A., Cevher, E., Pabuccuoğlu, S., & Özgümüş, S. (2018). pH sensitive functionalized hyperbranched polyester based nanoparticulate system for the receptor-mediated targeted cancer therapy. *International Journal of Polymeric Materials and Polymeric Biomaterials*, *68*(8), 1–16.

Barakat, N. S., & Ahmad, A. A. E. (2008). Diclofenac sodium loaded-cellulose acetate butyrate: Effect of processing variables on microparticles properties, drug release kinetics and ulcerogenic activity. *Journal of Microencapsulation*, *25*(1), 31–45.

Bauer, H. W., Klasser, M., Von Hanstein, K. L., Rolinger, H., Schladitz, G., Henke, H. D., … Steinbach, K. (1999). Oxaceprol is as effective as diclofenac in the therapy of osteoarthritis of the knee and hip. *Clinical Rheumatology*, *18*(1), 4–9.

Biehl, G., Bayer, I., & Schäferhoff, P. (1993). Therapie von Spondylarthrosen: Klinischer Vergleich von Oxaceprol mit Ibuprofen. *Extracta orthopaedica*, *16*, 18–22.

Chaudhary, H., & Kumar, V. (2014). Taguchi design for optimization and development of antibacterial drug-loaded PLGA nanoparticles. *International Journal of Biological Macromolecules*, *64*, 99–105.

Chereddy, K. K., Vandermeulen, G., & Préat, V. (2016). PLGA based drug delivery systems: Promising carriers for wound healing activity. *Wound Repair and Regeneration*, *24*(2), 223–236.

Corrigan, O. I., & Li, X. (2009). Quantifying drug release from PLGA nanoparticulates. *European Journal of Pharmaceutical Sciences*, *37*(3–4), 477–485.

Danhier, F., Ansorena, E., Silva, J. M., Coco, R., Le Breton, A., & Préat, V. (2012). PLGA-based nanoparticles: An overview of biomedical applications. *Journal of Controlled Release*, *161*(2), 505–522. https://doi.org/10.1016/j.jconrel.2012.01.043

Dillen, K., Vandervoort, J., Van den Mooter, G., & Ludwig, A. (2006). Evaluation of ciprofloxacin-loaded Eudragit® RS100 or RL100/PLGA nanoparticles. *International Journal of Pharmaceutics*, *314*(1), 72–82. https://doi.org/10.1016/j.ijpharm.2006.01.041

Ding, D., & Zhu, Q. (2018). Recent advances of PLGA micro/-nanoparticles for the delivery of biomacromolecular therapeutics. *Materials Science and Engineering: C*, *92*, 1041–1060. https://doi.org/10.1016/j.msec.2017.12.036

Ding, S., Serra, C. A., Vandamme, T. F., Yu, W., & Anton, N. (2018). Double emulsions prepared by two-step emulsification: History, state-of-the-art and perspective. *Journal of Controlled Release*. *92*, 1041–1060

Dong, Y., & Feng, S.-S. (2004). Methoxy poly(ethylene glycol)-poly (lactide) (MPEG-PLA) nanoparticles for controlled delivery of anticancer drugs. *Biomaterials*, *25*(14), 2843–2849. https://doi.org/10.1016/j.biomaterials.2003.09.055

Dunne, M., Corrigan, O. I., & Ramtoola, Z. (2000). Influence of particle size and dissolution conditions on the degradation properties of polylactide-co-glycolide particles. *Biomaterials*, *21*(16), 1659–1668. https://doi.org/10.1016/S0142-9612(00)00040-5

Durg, S., Lobo, M., Venkatachalam, L., Rao, G., & Bhate, J. (2019). A systematic review and meta-analysis of oxaceprol in the management of osteoarthritis: An evidence from randomized parallel-group controlled trials. *Pharmacological Reports*, *71*(2), 374–383. https://doi.org/10.1016/j.pharep.2018.12.010

England, C. G., Miller, M. C., Kuttan, A., Trent, J. O., & Frieboes, H. B. (2015). Release kinetics of paclitaxel and cisplatin from two and three layered gold nanoparticles. *European Journal of Pharmaceutics and Biopharmaceutics*, *92*, 120–129. https://doi.org/10.1016/j.ejpb.2015.02.017

Eren, F., Öksüz, S., Küçükodaci, Z., Kendırlı, M. T., Cesur, C., Alarçın, E., … Köse, G. T. (2016). Targeted mesenchymal stem cell and vascular endothelial growth factor strategies for repair of nerve defects with nerve tissue implanted autogenous vein graft conduits. *Microsurgery*, *36*(7), 578–585.

Gu, J., Chen, N., Ding, G., & Zhang, Z. (2011). Determination of oxaceprol in rat plasma by LC–MS/MS and its application in a pharmacokinetic study. *Journal of Pharmaceutical and Biomedical Analysis*, *54*(1), 173–178.

Gupta, H., Aqil, M., Khar, R. K., Ali, A., Bhatnagar, A., & Mittal, G. (2010). Sparfloxacin-loaded PLGA nanoparticles for sustained ocular drug delivery. *Nanomedicine: Nanotechnology, Biology and Medicine*, *6*(2), 324–333.

Harris, A., Schropp, A., & Messmer, K. (1998). Effects of oxaceprol on the microcirculation in ischemia/reperfusion injury. *European Journal of Medical Research*, *3*(4), 182–188.

He, Z., Wang, B., Hu, C., & Zhao, J. (2017). An overview of hydrogel-based intra-articular drug delivery for the treatment of osteoarthritis. *Colloids and Surfaces B: Biointerfaces*, *154*, 33–39. https://doi.org/10.1016/j.colsurfb.2017.03.003

Herrmann, G., Steeger, D., Klasser, M., Wirbitzky, J., Fürst, M., Venbrocks, R., … Parnham, M. J. (2000). Oxaceprol is a well-tolerated therapy for osteoarthritis with efficacy equivalent to diclofenac. *Clinical Rheumatology*, *19*(2), 99–104.

Ho, M. J., Kim, S. R., Choi, Y. W., & Kang, M. J. (2018). Recent advances in intra-articular drug delivery systems to extend drug retention in joint. *Journal of Pharmaceutical Investigation*, *49*(1), 1–7.

Holgado, M. A., Arias, J. L., Cózar, M. J., Alvarez-Fuentes, J., Ganan-Calvo, A. M., & Fernández-Arévalo, M. (2008). Synthesis of lidocaine-loaded PLGA microparticles by flow focusing: Effects on drug loading and release properties. *International Journal of Pharmaceutics*, *358*(1–2), 27–35.

Horisawa, E., Hirota, T., Kawazoe, S., Yamada, J., Yamamoto, H., Takeuchi, H., & Kawashima, Y. (2002). Prolonged anti-inflammatory action of DL-lactide/glycolide copolymer nanospheres containing betamethasone sodium phosphate for an intra-articular delivery system in antigen-induced arthritic rabbit. *Pharmaceutical Research*, *19*(4), 403–410.

Horisawa, E., Kubota, K., Tuboi, I., Sato, K., Yamamoto, H., Takeuchi, H., & Kawashima, Y. (2002). Size-dependency of DL-lactide/glycolide copolymer particulates for intra-articular delivery system on phagocytosis in rat synovium. *Pharmaceutical Research*, *19*(2), 132–139.

ICH Harmonised Tripartite Guideline. (2005). *Validation of analytical procedures: Text and methodology Q2 (R1)*. In International conference on harmonisation of technical requirements for registration of pharmaceuticals for human use.

Ionac, M., Parnham, M. J., Plauchithiu, M., & Brune, K. (1996). Oxaceprol, an atypical inhibitor of inflammation and joint damage. *Pharmacological Research*, *33*(6), 367–373.

Ji, Y., Wang, M., Liu, W., Chen, C., Cui, W., Sun, T., … Guo, X. (2017). Chitosan/nHAC/PLGA microsphere vehicle for sustained release of rhBMP-2 and its derived synthetic oligopeptide for bone regeneration. *Journal of Biomedical Materials Research Part A*, *105*(6), 1593–1606.

Jose, S., Sowmya, S., Cinu, T. A., Aleykutty, N. A., Thomas, S., & Souto, E. B. (2014). Surface modified PLGA nanoparticles for brain targeting of Bacoside-A. *European Journal of Pharmaceutical Sciences*, *63*, 29–35. https://doi.org/10.1016/j.ejps.2014.06.024

Kang, M. L., Ko, J. Y., Kim, J. E., & Im, G. I. (2014). Intra-articular delivery of kartogenin-conjugated chitosan nano/microparticles for cartilage regeneration. *Biomaterials*, *35*(37), 9984–9994. https://doi.org/10.1016/j.biomaterials.2014.08.042

Karagoz, H., Ulkur, E., Kerimoglu, O., Alarcin, E., Sahin, C., Akakin, D., & Dortunc, B. (2012). Vascular endothelial growth factor-loaded poly(lactic-co-glycolic acid) microspheres-induced lateral axonal sprouting into the vein graft bridging two healthy nerves: Nerve graft prefabrication using controlled release system. *Microsurgery*, *32*(8), 635–641. https://doi.org/10.1002/micr.22016

Kim, C., Jeon, O. H., Kim, D. H., Chae, J. J., Shores, L., Bernstein, N., … Elisseeff, J. H. (2016). Local delivery of a carbohydrate analog for reducing arthritic inflammation and rebuilding cartilage. *Biomaterials*, *83*, 93–101. https://doi.org/10.1016/j.biomaterials.2015.12.029

Kruger, K., Klasser, M., Mossinger, J., & Becker, U. (2007). Oxaceprol-A randomised, placebo-controlled clinical study in osteoarthritis with a non-conventional non-steroidal anti-inflammatory drug. *Clinical and Experimental Rheumatology*, *25*(1), 29–34.

Mainardes, R. M., & Evangelista, R. C. (2005). PLGA nanoparticles containing praziquantel: Effect of formulation variables on size distribution. *International Journal of Pharmaceutics*, *290*(1), 137–144. https://doi.org/10.1016/j.ijpharm.2004.11.027

Martinez, N. Y., Andrade, P. F., Durán, N., & Cavalitto, S. (2017). Development of double emulsion nanoparticles for the encapsulation of bovine serum albumin. *Colloids and Surfaces B: Biointerfaces*, *158*, 190–196.

Martins, C., Sousa, F., Araújo, F., & Sarmento, B. (2018). Functionalizing PLGA and PLGA derivatives for drug delivery and tissue regeneration applications. *Advanced Healthcare Materials*, *7*(1), 1701035.

Maudens, P., Seemayer, C. A., Thauvin, C., Gabay, C., Jordan, O., & Allémann, E. (2018). Nanocrystal–polymer particles: Extended delivery carriers for osteoarthritis treatment. *Small*, *14*(8), 1703108.

Morag, A., Kirchheiner, J., Rehavi, M., & Gurwitz, D. (2010). Human lymphoblastoid cell line panels: Novel tools for assessing shared drug pathways. *Pharmacogenomics*, *11*(3), 327–340.

Pawar, H. S., Francis, N. K., Hota, T., Peter, N., & Mitra, A. (2018). Comparative evaluation of therapeutic efficacy of intra-articular oxaceprol with conventional modalities in osteoarthritis animal model. *Clinical Rheumatology*, *37*(8), 2195–2201. https://doi.org/10.1007/s10067-018-4087-1

Rehman, M., Madni, A., Ihsan, A., Khan, W. S., Khan, M. I., Mahmood, M. A., … Shakir, I. (2015). Solid and liquid lipid-based binary solid lipid nanoparticles of diacerein: in vitro evaluation of sustained release, simultaneous loading of gold nanoparticles, and potential thermo-responsive behavior. *International Journal of Nanomedicine*, *10*, 2805–2814. https://doi.org/10.2147/ijn.s67147

Shabir, G. A. (2003). Validation of high-performance liquid chromatography methods for pharmaceutical analysis: Understanding the differences and similarities between validation requirements of the US Food and Drug Administration, the US Pharmacopeia and the International Conference on Harmonization. *Journal of Chromatography A*, *987*(1), 57–66. https://doi.org/10.1016/S0021-9673(02)01536-4

Sipahigil, O., Alarcin, E., Turkoglu, M., Dortunc, B., Karagoz, H., Ulkur, E., … Capan, Y. (2012). Characterization, cell proliferation and cytotoxicity evaluation of vascular endothelial growth factor loaded poly (lactic-co-glycolic acid) microspheres. *Nobel Medicus*, *8*(1), 77–82.

Sokol, M. B., Nikolskaya, E. D., Yabbarov, N. G., Zenin, V. A., Faustova, M. R., Belov, A. V., … Tereshchenko, O. G. (2018). Development of novel PLGA nanoparticles with co-encapsulation of docetaxel and abiraterone acetate for a highly efficient delivery into tumor cells. *Journal of Biomedical Materials Research Part B: Applied Biomaterials*. *107*(4), 1150–1158.

Song, X., Zhao, Y., Wu, W., Bi, Y., Cai, Z., Chen, Q., … Hou, S. (2008). PLGA nanoparticles simultaneously loaded with vincristine sulfate and verapamil hydrochloride: Systematic study of particle size and drug entrapment efficiency. *International Journal of Pharmaceutics*, *350*(1), 320–329. https://doi.org/10.1016/j.ijpharm.2007.08.034

Souillac, P., & Rytting, J. H. (1999). Characterization of delivery systems, differential scanning calorimetry. *Encyclopedia of Controlled Drug Delivery*, *1*, 212–227.

Sulistio, A., Reyes-Ortega, F., D'Souza, A. M., Ng, S. M. Y., Valade, D., Quinn, J. F., … Qiao, G. (2017). Precise control of drug loading and release of an NSAID–polymer conjugate for long term osteoarthritis intra-articular drug delivery. *Journal of Materials Chemistry B*, *5*(31), 6221–6226.

Tansık, G., Yakar, A., & Gündüz, U. (2014). Tailoring magnetic PLGA nanoparticles suitable for doxorubicin delivery. *Journal of Nanoparticle Research*, *16*(1), 2171.

Tellier, L. E., Treviño, E. A., Brimeyer, A. L., Reece, D. S., Willett, N. J., Guldberg, R. E., & Temenoff, J. S. (2018). Intra-articular TSG-6 delivery from heparin-based microparticles reduces cartilage damage in a rat model of osteoarthritis. *Biomaterials Science*, *6*(5), 1159–1167.

Vagt, C. W., Kaiser, T., & Leineweber, G. (1990). Wirksamkeitsvergleich der oralen Therapie mit Oxazeprol versus Ibuprofen bei Gonarthrose und Coxarthrose. *Rheuma*, *10*, 263–267.

Veihelmann, A., Hofbauer, A., Refior, H. J., & Messmer, K. (2001). Oxaceprol, an atypical inhibitor of inflammation, reduces leukocyte adherence in mouse antigen-induced arthritis. *Acta Orthopaedica Scandinavica*, *72*(3), 293–298.

Vincent, M., Oved, K., Morag, A., Pasmanik-Chor, M., Oron-Karni, V., Shomron, N., & Gurwitz, D. (2012). Genome-wide transcriptomic variations of human lymphoblastoid cell lines: Insights from pairwise gene-expression correlations. *Pharmacogenomics*, *13*(16), 1893–1904.

Zhang, W., Ouyang, H., Dass, C. R., & Xu, J. (2016). Current research on pharmacologic and regenerative therapies for osteoarthritis. *Bone Research*, *4*, 15040. https://doi.org/10.1038/boneres.2015.40

SUPPORTING INFORMATION

Additional supporting information may be found online in the Supporting Information section at the end of this article.

How to cite this article: Alarçin E, Demirbağ Ç, Karsli-Ceppioglu S, Kerimoğlu O, Bal-Ozturk A. Development and characterization of oxaceprol-loaded poly-lactide-co-glycolide nanoparticles for the treatment of osteoarthritis. *Drug Dev Res*. 2020;1–10. https://doi.org/10.1002/ddr.21642